AAC Journals.ASM.org

Rapid Conversion of *Pseudomonas aeruginosa* to a Spherical Cell Morphotype Facilitates Tolerance to Carbapenems and Penicillins but Increases Susceptibility to Antimicrobial Peptides

Leigh G. Monahan,[a] Lynne Turnbull,[a] Sarah R. Osvath,[a] Debra Birch,[b] Ian G. Charles,[a] Cynthia B. Whitchurch[a]

The ithree institute, University of Technology Sydney, Ultimo, NSW, Australia[a]; Microscopy Unit, Faculty of Science, Macquarie University, North Ryde, NSW, Australia[b]

The Gram-negative human pathogen *Pseudomonas aeruginosa* tolerates high concentrations of β-lactam antibiotics. Despite inhibiting the growth of the organism, these cell wall-targeting drugs exhibit remarkably little bactericidal activity. However, the mechanisms underlying β-lactam tolerance are currently unclear. Here, we show that *P. aeruginosa* undergoes a rapid *en masse* transition from normal rod-shaped cells to viable cell wall-defective spherical cells when treated with β-lactams from the widely used carbapenem and penicillin classes. When the antibiotic is removed, the entire population of spherical cells quickly converts back to the normal bacillary form. Our results demonstrate that these rapid population-wide cell morphotype transitions function as a strategy to survive antibiotic exposure. Taking advantage of these findings, we have developed a novel approach to efficiently kill *P. aeruginosa* by using carbapenem treatment to induce *en masse* transition to the spherical cell morphotype and then exploiting the relative fragility and sensitivity of these cells to killing by antimicrobial peptides (AMPs) that are relatively inactive against *P. aeruginosa* bacillary cells. This approach could broaden the repertoire of antimicrobial compounds used to treat *P. aeruginosa* and serve as a basis for developing new therapeutic agents to combat bacterial infections.

Pseudomonas aeruginosa is a major human pathogen and a leading cause of hospital-acquired infections. *P. aeruginosa* infections are difficult to eradicate and are often fatal, which is in part due to the organism's high intrinsic resistance to a variety of different antimicrobials (1). The mechanisms underlying intrinsic antibiotic resistance in *P. aeruginosa* are largely well understood. However, an important and as yet unexplained observation is the ability of *P. aeruginosa* to survive in the presence of high concentrations of the cell wall-targeting β-lactam antibiotics.

β-Lactams are a broad class of antibiotics that include penicillin derivatives, cephalosporins, monobactams, and carbapenems. They are the most widely used group of antibiotics in the world (2) and mediate bacterial killing primarily by inhibiting the enzymes, known as penicillin-binding proteins (PBPs), that catalyze the formation of peptidoglycan cross-links in the bacterial cell wall (3). β-Lactam drugs typically exhibit bactericidal activity against susceptible organisms (4), and this is often associated with changes in bacterial morphology and the formation of spherical or filamentous cells that are prone to lysis (3, 5–8).

Interestingly, despite inhibiting cell growth, β-lactams have been found to have very little bactericidal activity against *P. aeruginosa* (9–13). This intrinsic tolerance of β-lactams likely accounts for the fact that when *P. aeruginosa* infections are treated, optimal microbiological outcomes occur when β-lactam concentrations are maintained at 4 to 6.6 times the MIC throughout the majority of the dosing period (13). Furthermore, β-lactam tolerance by *P. aeruginosa* can lead to the emergence of spontaneous β-lactam-resistant strains (12, 14). Thus, β-lactam tolerance provides significant challenges for clinicians when treating *P. aeruginosa* infections. The mechanisms underlying this tolerance, however, are unclear.

Here, we show that tolerance of *P. aeruginosa* to several β-lactams, including carbapenems and a penicillin derivative, is mediated by a rapid population-wide transition to a viable, cell wall-defective spherical form. We demonstrate that these spherical cells can survive in the presence of antibiotic and quickly revert to the normal bacillary mode of growth following its removal. Our results indicate that transition to the spherical cell morphotype likely does not require the acquisition of specific mutations but rather is an intrinsic response to antibiotic exposure that serves as a survival strategy. Significantly, we further demonstrate that *P. aeruginosa* can be efficiently killed by combining the β-lactam meropenem with antimicrobial peptides that show little to no activity against bacillary cells of *P. aeruginosa*. We propose that such combination treatments could provide a novel approach for antibacterial therapy.

MATERIALS AND METHODS

Bacterial strains, media, and growth conditions. The *P. aeruginosa* strains used in this study were PA14, PAO1, PA103, PAK, ATCC 27853, PAE27 (otitis externa isolate; Gribbles Pathology, Melbourne, Australia), and PA911 (cystic fibrosis lung isolate; Monash Medical Centre, Melbourne, Australia). All experiments were performed with strain PA14 unless otherwise indicated. Cells were grown either in cation-adjusted Mueller-Hinton broth (CAMHB) (Fig. 1), synthetic cystic fibrosis sputum medium (15) (see Fig. S1A in the supplemental material), fetal bovine serum (see Fig. S1B in the supplemental material), or CAMHB supplemented with 0.5 M sucrose (Fig. 2 through 7; also see Fig. S2 and S3 in the supplemental material). To induce spherical cell formation, cultures were

Received 31 August 2013 Returned for modification 27 October 2013
Accepted 28 December 2013
Published ahead of print 13 January 2014
Address correspondence to Cynthia B. Whitchurch, cynthia.whitchurch@uts.edu.au.
Supplemental material for this article may be found at http://dx.doi.org/10.1128/AAC.01901-13.

doi:10.1128/AAC.01901-13

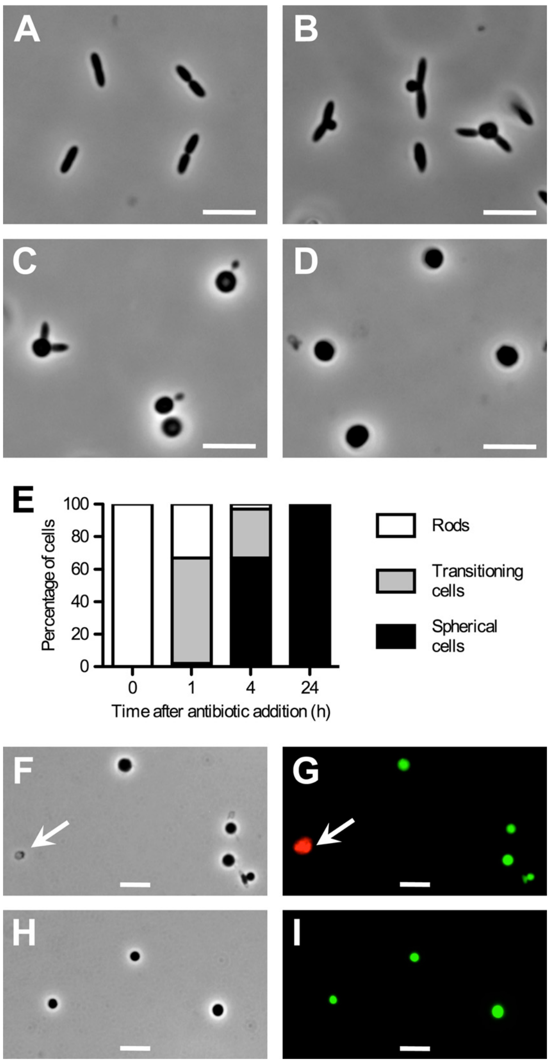

FIG 1 *P. aeruginosa* rapidly converts to spherical cells in response to a β-lactam antibiotic. PA14 cells cultured in cation-adjusted Mueller-Hinton broth (CAMHB) were treated with meropenem (5× MIC) and visualized by phase-contrast or fluorescence (LIVE/DEAD) microscopy. (A through D) Phase-contrast images taken immediately prior to meropenem addition (A) and after 1 h (B), 4 h (C), and 24 h (D) in the presence of the drug. (E) Proportion of rods, spherical cells, and transitioning cells in the population over time. A total of 200 cells were scored from phase-contrast micrographs at each time point from 2 experiments. (F through I) LIVE/DEAD viability staining of meropenem-treated cells after 24 h. Cells were grown in CAMHB (F through G) or CAMHB supplemented with 0.5 M sucrose (H through I). Samples were costained with SYTO9 (live, green) and propidium iodide (dead, red) and visualized by phase-contrast microscopy (F and H) and wide-field fluorescence microscopy (G and I). Arrows point to lysed cells. Scale bars, 5 μm.

grown to the early exponential phase at 37°C with vigorous shaking, antibiotic was added, and cells were then incubated without shaking at 37°C. For reversion, spherical cells were pelleted by centrifugation at 3,000 × *g* for 10 min, resuspended in antibiotic-free media, and grown with static incubation at 37°C. Antibiotics were used at 5× MIC, as determined against strain PA14 using standard methods (16). MIC values for PA14 were as follows: meropenem, 1 μg/ml; imipenem, 2 μg/ml; and carbenicillin, 128 μg/ml. MIC values for meropenem were also determined against each strain used in the study and were found to be between 1 and 2 μg/ml for all strains.

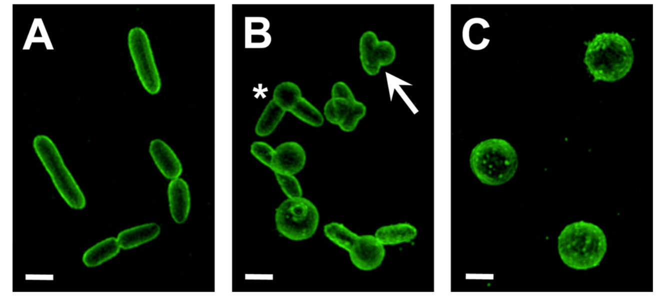

FIG 2 Superresolution 3D-SIM microscopy showing the transition of *P. aeruginosa* to meropenem-induced spherical cells. Following treatment with meropenem, PA14 cells were stained with membrane dye FM1-43 and visualized by 3D-SIM. Images were acquired at 0 h (A), 2 h (B), and 24 h (C) after meropenem addition. The asterisk highlights a developing spherical cell that is fully surrounded by membrane. The arrow indicates a cell at an earlier stage of the transition, containing a surface bulge that is not yet membrane enclosed. Scale bars, 1 μm.

Phase-contrast and fluorescence microscopy. To prepare samples for phase-contrast imaging, a 1.0 × 1.0-cm square well was set up on the surface of a glass microscope slide by attaching a 25-μl Gene Frame (ABgene). The well was filled with 25 μl of culture and a coverslip was placed on top. For fluorescence microscopy (LIVE/DEAD staining and superresolution three-dimensional structured illumination microscopy [3D-SIM]), 200 μl of cells was applied to a 35-mm sterile glass bottom

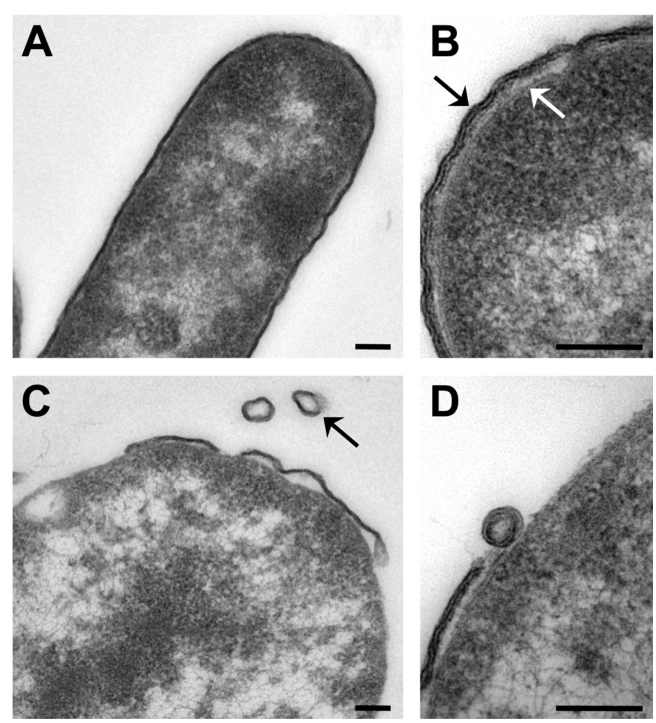

FIG 3 Meropenem-induced spherical cells of *P. aeruginosa* have a compromised cell envelope. Transmission electron microscopy (TEM) was performed on thin sections of PA14 cells immediately prior to the addition of meropenem (A and B) and after 24 h in the presence of the drug (C and D). Panels B and D are shown at high magnification to illustrate the cell envelope structure, revealing an intact outer membrane (black arrow) and inner membrane (white arrow) in the bacillary form (B) and a clearly disrupted outer membrane in the spherical cell (D). The arrow in panel C indicates a vesicle that appears to have formed from detached outer membrane material. Scale bars, 100 nm.

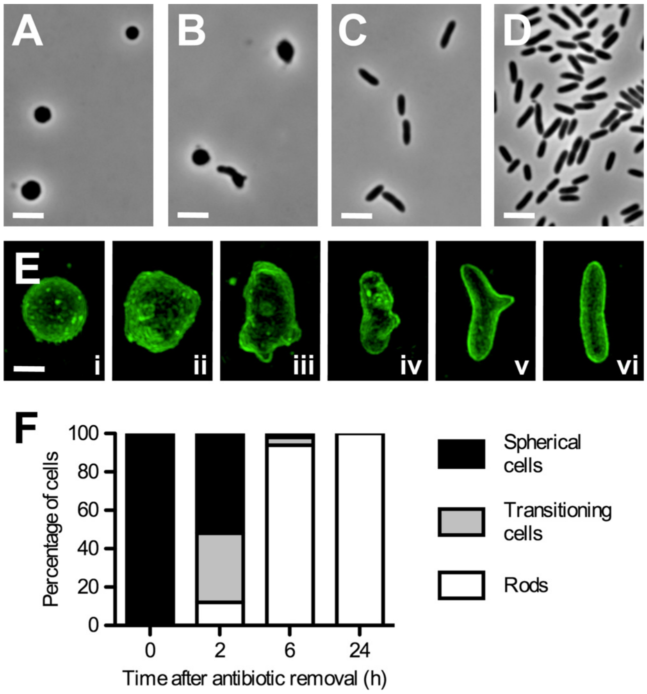

FIG 4 Spherical *P. aeruginosa* cells rapidly revert to normal rods in the absence of antibiotic. Meropenem-induced spherical cells of PA14 were resuspended in antibiotic-free media and visualized by phase-contrast microscopy or 3D-SIM. (A through E) Phase-contrast images taken at 0 h (A), 2 h (B), 6 h (C), and 24 h (D) after removal of meropenem. (E) 3D-SIM images of FM1-43 stained cells captured at various stages in the transition from spherical cells (i) to normal rods (vi). (F) Proportions of spherical cells, rods, and transitioning cells in the population over time. A total of 200 cells were scored from phase-contrast micrographs at each time point from 2 experiments. Scale bars, 5 μm (A through D) or 1 μm (E).

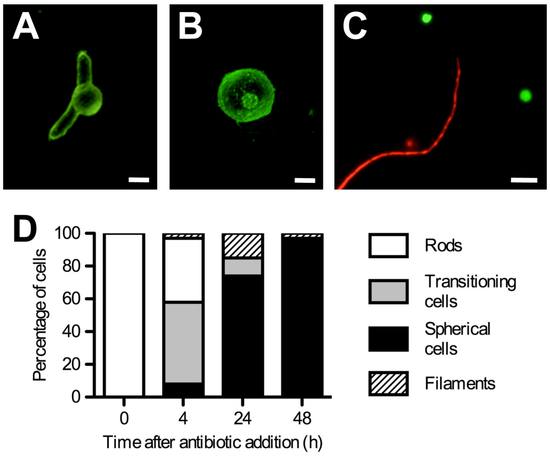

FIG 5 Spherical cells induced by carbenicillin. (A through B) 3D-SIM images of PA14 cells stained with membrane dye FM1-43 after 2 h (A) and 24 h (B) in the presence of carbenicillin. (C) LIVE/DEAD viability staining of carbenicillin-treated cells after 24 h, showing viable spherical cells and a dead filamentous cell. Cells were costained with SYTO9 (live, green) and propidium iodide (dead, red) and visualized by wide-field fluorescence microscopy. (D) Proportions of rods, spherical cells, transitioning cells, and filaments in the population over time. A total of 200 cells were scored from phase-contrast micrographs at each time point. Scale bars, 1 μm (A through B) or 5 μm (C).

FluoroDish (World Precision Instruments). Membrane stain FM1-43FX (5 μg/ml; Life Technologies) was added to the sample before applying to the dish for 3D-SIM. Syto9 (5 μM; Life Technologies) and propidium iodide (30 μM; BD) were added for LIVE/DEAD staining.

An Olympus IX71 wide-field inverted microscope was used for phase-contrast imaging, a Zeiss Axioplan 2 fluorescence microscope was used for imaging of LIVE/DEAD-stained cells, and a DeltaVision OMX-Blaze (Applied Precision, Inc.) was used for 3D-SIM (17). Images were processed as described previously (17), analyzed, and presented using AnalySIS Research Pro (Olympus), AxioVision (Zeiss), or Imaris (Bitplane) software.

Transmission electron microscopy. To prepare samples for transmission electron microscopy (TEM), cells were pelleted by centrifugation at 3,000 × *g* for 10 min and resuspended in a fixative solution of 2% glutaraldehyde in phosphate-buffered saline (PBS) (0.1 M [pH 7.2]) containing 0.1 M sucrose. Cells were fixed overnight at 4°C and then washed three times in PBS. Cell pellets were embedded in 1% low-melting-temperature agarose (J. T. Baker, Inc.) and agarose blocks were cut into 1-mm cubes, transferred to glass vials, and postfixed in 1% osmium tetroxide (OsO_4) in PBS for 1 h at room temperature. Following postfixation, samples were washed in distilled water three times for 5 min each wash and immersed in 2% aqueous uranyl acetate for 30 min. Cell pellets were dehydrated through a graded series of ethanols (50 to 100%), infiltrated, and subsequently embedded in LR White resin (London Resin Company). Ultrathin (70-nm) sections were cut using a Reichert ultramicrotome (Ultracut S; Leica Microsystems) and mounted onto pioloform-coated, 300-mesh, thin-bar copper grids. Grids were stained with saturated aqueous uranyl acetate (7.7%) for 30 min and Reynold's lead citrate for 4 min. Samples were examined using a Philips CM0 transmission electron microscope equipped with a Megaview III TEM charge-coupled device (CCD) camera and iTEM image capture software (Olympus). Digital images were processed for publication using Adobe Photoshop CS version 8.0 (Adobe Systems). All TEM materials were supplied from ProSciTech, Australia.

Viability assays. To estimate the number of viable cells in culture, 10-fold dilutions were plated in triplicate onto LB medium containing 1.6% agar (without antibiotics) and incubated overnight at 37°C. Colonies were counted, and viability was calculated as the number of CFU per ml of culture.

RESULTS

***P. aeruginosa* cells rapidly convert to a viable spherical morphotype when treated with meropenem.** As an initial approach to understand β-lactam tolerance by *P. aeruginosa*, we monitored *P. aeruginosa* cells under the microscope following treatment with meropenem, a broad-spectrum carbapenem antibiotic that is commonly used to treat *P. aeruginosa* infections in humans. It has been noted in previous studies that *P. aeruginosa* cells switch to a spherical morphology when exposed to meropenem (7, 8). We hypothesized that this spherical morphotype may be a viable alternative form of the bacterium that mediates survival in the presence of the antibiotic.

To test this, *P. aeruginosa* strain PA14 was first cultured in a standard laboratory growth medium (cation-adjusted Mueller-Hinton broth) and treated with a clinically relevant dose of meropenem (5× MIC). Cells were then visualized at regular intervals using conventional phase-contrast microscopy. In the presence of meropenem, we observed a rapid and efficient conversion of the entire population from normal rod-shaped cells to apparently spherical cells (Fig. 1A to E). Just 1 h after the addition of the antibiotic, a large proportion of cells (65%) had clearly begun transitioning to the spherical morphology. Most cells (67%) had completed the transition by 4 h, and after 24 h the entire population consisted only of spherical cells (Fig. 1E). To determine if

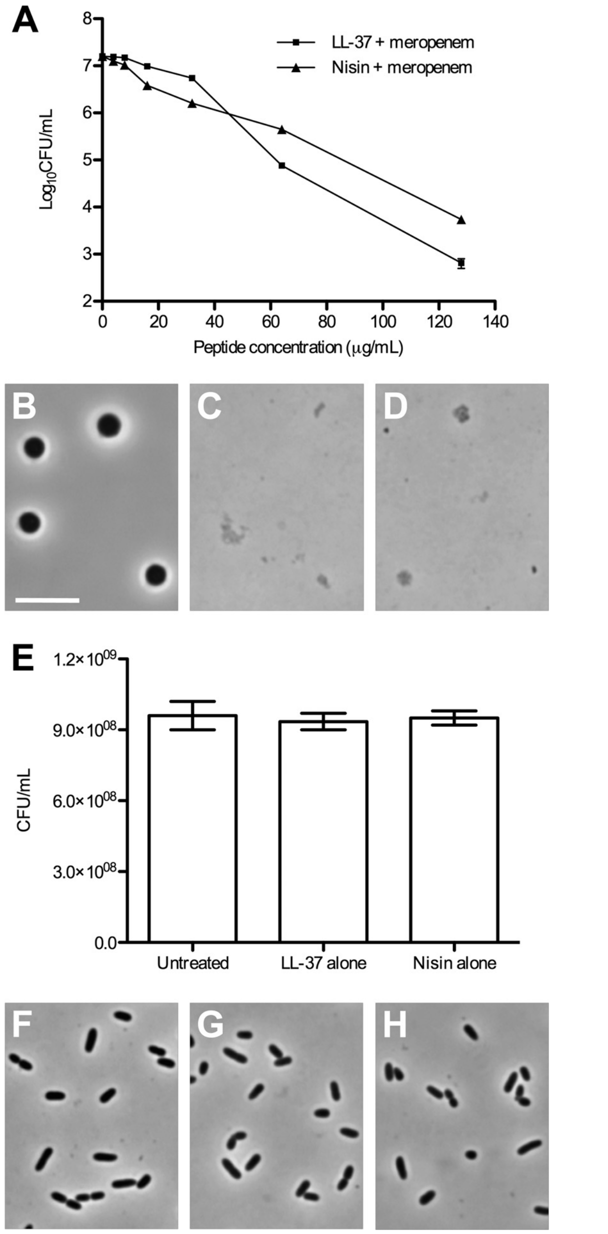

FIG 6 AMPs selectively kill meropenem-induced spherical cells of *P. aeruginosa*. (A) Viable cell counts after treatment of PA14 for 24 h with a combination of meropenem (5 μg/ml) and either LL-37 or nisin (0 to 128 μg/ml). (B through D) Representative phase-contrast images of cells treated under the same conditions as those shown in panel A. (B) Meropenem-only control (no peptide), showing intact spherical cells. (C) LL-37 (128 μg/ml) with meropenem. (D) Nisin (128 μg/ml) with meropenem. Cellular debris can be seen in place of intact cells for both AMP-meropenem combinations. (E) Viability counts for untreated cells and cells treated with LL-37 or nisin alone (128 μg/ml). (F through H) Corresponding phase-contrast images. (F) Untreated control, showing normal rod-shaped cells. (G) LL-37. (H) Nisin. Neither AMP alone appears to have any effect on cellular morphology. Scale bar, 5 μm. For panels A and E, one representative data set is shown from duplicate (A) or triplicate (E) experiments. Error bars correspond to the standard errors of the means for triplicate measurements.

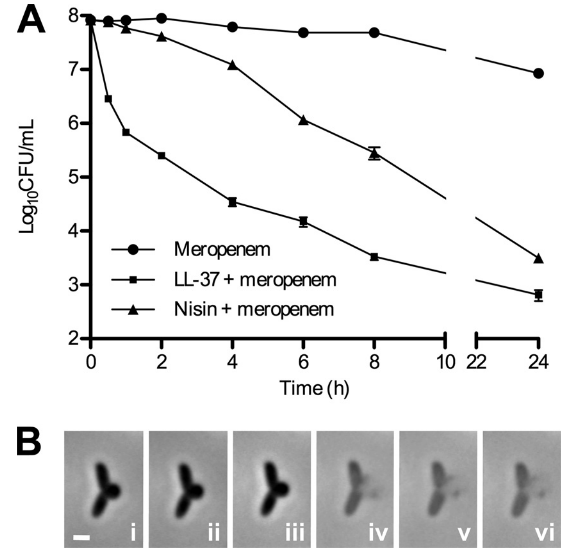

FIG 7 Meropenem and AMP combinations induce rapid cell death. (A) Time-kill assay. Viable cell counts were measured at regular intervals after the addition of meropenem (5 μg/ml), both alone and in combination with LL-37 or nisin (128 μg/ml), to a culture of PA14 cells. One representative data set from duplicate experiments is shown. Error bars correspond to the standard error of the mean for triplicate measurements. (B) Time-lapse microscopy capturing the peptide-mediated death of a developing spherical cell. PA14 cells were treated with meropenem (5 μg/ml) for 1 h to induce a partial transition to the spherical state. LL-37 (128 μg/ml) was then added, and phase-contrast images were collected at 2-s intervals over a period of 30 min. In the example shown, the image in panel i was acquired 13 min after the addition of the peptide, and each subsequent image after an additional 2 s. A total of 13 individual cell death events were observed over four separate experiments. Scale bar, 1 μm.

these spherical cells were viable, we costained PA14 with the fluorescent dyes Syto9 and propidium iodide after 24-h exposure to meropenem. This approach differentiates viable cells, which stain only with Syto9 (green), from dead cells, which also stain with propidium iodide (red) (Fig. 1F and G). These assays showed that the vast majority of spherical cells in the population (84%) were viable and thus tolerated exposure to 5× MIC of the antibiotic.

The remaining 16% of cells were lysed and were distinguishable from viable cells not only by LIVE/DEAD staining but also by a characteristic ghostlike appearance in phase-contrast images (Fig. 1F, arrow). Interestingly, we found that the addition of 0.5 M sucrose to the growth medium as an osmoprotectant reduced the number of lysed cells from 16% to 3% after 24-h exposure to meropenem (Fig. 1H and I). Osmoprotection was clearly not essential for spherical cell formation or viability; however, unless otherwise indicated, we chose to add 0.5 M sucrose to the growth medium in subsequent experiments (Fig. 2 to 7) simply to minimize the small amount of cell lysis observed in standard laboratory broth.

Importantly, we also tested whether spherical cells can form under conditions relevant to infection and the *in vivo* environment. To this end, PA14 cells were treated with meropenem (5× MIC) in a synthetic sputum medium designed to mimic the cystic fibrosis lung (15), as well as in fetal bovine serum. Note that sucrose was not added to these media. In both synthetic sputum and fetal bovine serum we observed rapid transitions of the cellular population from rods to spherical cells following treatment with meropenem, similar to that seen in standard growth media (see Fig. S1 in the supplemental material). Therefore, our results demonstrate that *P. aeruginosa* spherical cells form in response to meropenem exposure under physiologically relevant conditions.

To confirm the spherical shape of meropenem-treated cells, we used 3D-structured illumination microscopy (3D-SIM), a super-resolution fluorescence technique that enables genuine 3D images of bacterial cells and reveals morphological details not visible with conventional microscopy through increases in both lateral and axial resolution (18) (Fig. 2). We also used 3D-SIM to examine the transition from rod to sphere and found that it begins with the emergence of a small membrane protrusion on the cell surface (Fig. 2B). This gradually bulges out to form a larger sphere, which becomes completely enclosed in its own membrane. The original rod then lyses, leaving a mature, spherical cell (Fig. 2B and C).

***P. aeruginosa* spherical cells have a defective cell wall and disrupted outer membrane.** The bacterial cell wall is a key structural feature of the cell that determines its shape and serves as an important osmotic barrier to the external environment. The loss of cell shape observed after meropenem treatment of *P. aeruginosa*, together with the slight osmosensitivity of the resulting spherical cells (see above), strongly suggests that these cells lack a functional cell wall. In addition, we found that spherical cells rapidly burst when placed directly between a microscope slide and a coverslip, indicating a mechanical fragility consistent with loss of integrity in the cell envelope.

To further examine the cell envelope structure of the spherical cell morphotype, we performed transmission electron microscopy (TEM) on thin sections of PA14 cells after 24-h exposure to meropenem. We also examined untreated cells as controls, and as expected, these cells exhibited a regular double-membrane cell envelope structure characteristic of Gram-negative bacteria (Fig. 3A and B). In spherical cells, however, the outer membrane was clearly disrupted in all cells examined (Fig. 3C and D) (82 cells were analyzed in total). While fragments of outer membrane remained associated with the cell (Fig. 3C), there were extensive regions in which the inner membrane appeared to be exposed on the cell surface. Interestingly, membrane vesicles were often observed to form, apparently from outer-membrane material that had detached from the cell envelope (Fig. 3C and D). Taken together, these results indicate that *P. aeruginosa* cells can convert to an alternative form deficient in an intact cell wall and outer membrane when challenged with a cell wall-targeting antibiotic.

The transition to spherical cells is readily reversible. To test whether *P. aeruginosa* PA14 spherical cells induced by meropenem treatment can revert to normal rod-shaped cells in the absence of antibiotic selection, we resuspended spherical cells formed after 24-h exposure to meropenem in fresh media lacking the drug. Cells were then visualized at regular intervals by phase-contrast microscopy and 3D-SIM. Under these conditions, we observed a rapid population-wide transition of the cellular population from spherical cells back to normal bacillary cells (Fig. 4). The first visible sign of this reversion was a change from a spherical to an ellipsoid morphology, which could be seen in some cells after just 30 min in the absence of drug. This was followed by a gradual elongation in cell length and reduction in width to produce a normal cylindrical cell. High-resolution 3D-SIM images showed that the cell surface was highly irregular, sometimes even branched, during this reversion process but ultimately became smooth and uniform as the normal cell wall was restored (Fig. 4E). After 6 h in the absence of antibiotic, the vast majority of the cellular population (>90%) had completed the transition to rods (Fig. 4F). These cells were able to grow and divide normally, as evidenced by a rapid increase in the density of cells in culture following reversion to the rod shape (Fig. 4C and D). This indicates that the transition to spherical cells following exposure to meropenem is readily reversible.

Spherical cell formation is a conserved mechanism of meropenem tolerance. Importantly, we observed that the ability to transition into and out of the spherical cell state occurred independently of strain background. Identical responses to meropenem treatment were seen for a wide variety of *P. aeruginosa* strains, including well-known lab strains (PA14, PAO1, PA103, PAK, and ATCC 27853) and recent clinical isolates (data not shown). This observation, along with the sheer speed, efficiency, and reversibility of the transition from rods to spherical cells, indicates that the formation of spherical cells in *P. aeruginosa* does not depend on the acquisition of chromosomal mutations. Rather, our results suggest that spherical cell formation is an intrinsic protective response. By undergoing rapid *en masse* phenotypic transitions between bacillary and spherical cell morphotypes, the vast majority of the *P. aeruginosa* population is able to survive exposure to meropenem and is poised to transition to the bacillary form when antibiotic levels are reduced.

Penicillins and carbapenems induce spherical cell-mediated antibiotic tolerance. Having determined that *P. aeruginosa* PA14 cells quickly convert to a spherical cell morphotype when treated with meropenem, we were interested to determine whether other cell wall-targeting antibiotics can elicit a similar response. Interestingly, *P. aeruginosa* has previously been shown to induce "spheroplasts" in response to carbenicillin (19), a penicillin derivative, and we reasoned that these spherical cells facilitate tolerance to the drug. We found that following treatment of PA14 with carbenicillin (5× MIC), a large proportion of cells indeed converted to spherical cells and did so via the same morphological pathway that we observed in response to meropenem exposure (Fig. 5). In contrast to meropenem, however, some cells became filamentous rather than converting to the spherical cell state (Fig. 5). While filamentation is a common phenotype associated with β-lactam treatment in rod-shaped bacteria (3, 20), we found that the *P. aeruginosa* filamentous cells arising under these conditions tended to lyse. LIVE/DEAD staining with Syto9 and propidium iodide showed that the filamentous cells stained with propidium iodide, indicating that they were nonviable (Fig. 5C), whereas the spherical cell morphotypes stained only with Syto9 and were therefore viable. As was observed after removal of meropenem, the population of carbenicillin-induced spherical cells rapidly reverted to normal bacillary cells when resuspended in fresh media lacking the antibiotic (data not shown).

We also examined the effect of imipenem (5× MIC) on *P. aeruginosa* PA14 cells. Like meropenem, imipenem is a carbapenem antibiotic, and we found that this also induced a rapid and reversible transition of the entire cellular population to spherical cells (see Fig. S2 in the supplemental material). Taken together, these results demonstrate that spherical cell-mediated antibiotic tolerance in *P. aeruginosa* can occur in response to β-lactams from at least two classes.

Meropenem-induced spherical cells are efficiently killed by antimicrobial peptides. Having established that *P. aeruginosa* cells convert very rapidly and efficiently to cell wall-deficient spherical cells when treated with β-lactam antibiotics, we hypothesized that the combination of a β-lactam that induces spherical cell formation with a drug that kills spherical cells could be feasible as a new and effective treatment approach for *P. aeruginosa* infections. One class of compounds that we reasoned might exhibit strong spherical cell killing activity were antimicrobial peptides (AMPs). These compounds function by direct interaction with membrane lipids and are thought to induce cell death through the formation of pores in the cytoplasmic membrane (21). Our TEM images show that there are vast stretches of cytoplasmic membrane exposed on the surface of spherical cells (Fig. 3), which should therefore be much more accessible to AMPs. Importantly, AMPs tend to have only weak antimicrobial activities against normal bacillary cells of *P. aeruginosa* under physiological conditions (22).

To test our hypothesis, cultures of *P. aeruginosa* PA14 were treated with a combination of meropenem to induce spherical cell formation (at a fixed concentration of 5 μg/ml) and one of the AMPs, LL-37 or nisin (at various concentrations between 0 and 128 μg/ml). After 24 h in the presence of the drug combinations, viable cell counts were determined by serial dilution and plating. While meropenem alone produced viable spherical cells, the addition of LL-37 or nisin markedly reduced viability (Fig. 6A). In fact, at the highest AMP concentration tested (128 μg/ml), viable cell counts were >3- to 4-log lower than those of the meropenem-only control. Fifty-percent inhibitory concentration (IC_{50}) values were 16 μg/ml for nisin and 32 μg/ml for LL-37 in combination with meropenem. The strong bactericidal activity of the meropenem-AMP combinations was further highlighted by a distinct absence of intact cells under the microscope, replaced with what appeared to be cellular debris (Fig. 6B to D). Importantly, under our assay conditions the AMPs alone (LL-37 or nisin) showed no detectable antibacterial ability (Fig. 6E to H) even at the highest concentration tested (128 μg/ml). This is consistent with the high MIC values recently reported for LL-37 against PA14 cells under similar conditions (23) (112 to 225 μg/ml). These observations suggest, as predicted, that AMPs are more effective against spherical cells than normal bacillary cells, which we further confirmed by demonstrating that the AMPs can efficiently kill preformed *P. aeruginosa* spherical cells (see Fig. S3 in the supplemental material).

Finally, time-kill assays were performed with PA14 to examine the rate of meropenem/AMP-induced cell death (Fig. 7A). Both LL-37 and nisin triggered a rapid decline in viability when administered in combination with meropenem. A 100-fold reduction of viable cell counts relative to the meropenem-only control was observed within just 1 h for LL-37 and 8 h for nisin, and by 24 h viability was reduced by 4 to 5 log for both AMP-meropenem combinations. Interestingly, the rapid killing by LL-37 suggests that only a partial transition of the cell to the spherical cell state is required for the AMP to mediate killing. We confirmed this for LL-37 using time-lapse microscopy, which showed that the peptide causes the cell to burst at the site of spherical cell formation (Fig. 7B).

DISCUSSION

Currently, there is a desperate need for innovative approaches to antimicrobial therapy. This stems from a relentless rise in the emergence of antibiotic-resistant bacteria, a lack of new antibiotic classes in the pharmaceutical pipeline, and greatly reduced investment within the pharmaceutical sector (24–26). Our data show that it is possible to effectively kill bacteria by turning their own biological responses against them, namely, by using drug combinations that induce the cell to transition to an alternative form and then exploiting the inherent weaknesses of that form. Drug combinations are commonly used in medicine to enhance the effectiveness of existing antibiotics (24) and represent a promising avenue for the development of new treatments (27–29) with reduced rates of resistance (30). In this study, we have shown that combinations of meropenem with the AMPs LL-37 or nisin are potently bactericidal against *P. aeruginosa* at concentrations where each drug alone has negligible bactericidal activity. Our findings provide a platform to identify novel antibacterial drug combinations that induce and target spherical cells in a directed and cost-effective manner.

Significantly, our observations suggest that the ability to switch between bacillary and spherical cell morphotypes is a response to stress invoked by exposure to β-lactam antibiotics. Transition of *P. aeruginosa* to the spherical state occurred rapidly in response to β-lactams from the carbapenem and penicillin classes and was found to be independent of genetic background. These results suggest that spherical cell formation may be an intrinsic developmental response of *P. aeruginosa* that is induced by antibiotic treatment. While the production of spherical cells by carbapenems and penicillins has been reported previously (7, 8, 19), our observations show for the first time that spherical cell formation is reversible and occurs readily under physiological conditions, indicating that this response may serve as a genuine mechanism of drug tolerance.

We propose that spherical cell-mediated β-lactam tolerance may underlie many of the pharmacodynamic challenges associated with β-lactam treatment of *P. aeruginosa* infections (12–14), at least in the case of carbapenems and penicillins. *P. aeruginosa* infections are notoriously difficult to treat and are often chronic or recurrent in nature, particularly in immunocompromised patients (31). It is tempting to speculate that the transition of *P. aeruginosa* to a viable alternative spherical cell morphotype during exposure to β-lactams could lead to prolonged or recurrent infections by allowing the bacterium to survive *in vivo* over the course of antibiotic treatment and then to revert to the bacillary form when antibiotic therapy is ceased.

Significantly, spherical cell formation may also play an important role in the emergence of β-lactam resistance. Spontaneous β-lactam-resistant mutants of *P. aeruginosa* are known to arise quite readily *in vitro* during antibiotic treatment (12, 14). Here we have shown that *P. aeruginosa* can undergo *en masse* transition to cell wall-defective spherical cells under these conditions. While in the spherical form, the population would be well poised to acquire β-lactam resistance, by either mutation or lateral gene transfer (1), which would enable reversion to the bacillary form and rapid cell proliferation. Consistent with this idea, early studies on carbenicillin-induced spheroplasts of *P. aeruginosa* showed that cells spontaneously reverted to rods after extended exposure to the drug (5 to 8 days), and that the MIC of carbenicillin increased as much as 150-fold following reversion (19, 32). Critically, we now show that a carbapenem in combination with antimicrobial peptides induces rapid killing of *P. aeruginosa* cells. This type of approach would severely limit the potential for acquiring resistance during β-lactam therapy.

A classic problem in population and evolutionary biology is to understand how a population copes with environmental changes that challenge survival. Common strategies that enable survival of antibiotic exposure by bacterial populations include selection of a subpopulation that has a fitness advantage that can arise through mutation, stochastic phenotypic heterogeneity, or regulated responses (33). Our observations suggest that tolerance to β-lactam exposure by *P. aeruginosa* can occur through an adaptive response that involves *en masse* phenotypic transitions between bacillary cells and spherical cells with defective cell walls. Therefore, population-wide morphotype transitions add to the repertoire of strategies that can be employed by bacteria to survive exposure to β-lactam antibiotics.

ACKNOWLEDGMENTS

C.B.W. was supported by an Australian National Health and Medical Research Council Senior Research Fellowship (571905). L.G.M. was supported by an ithree institute Postdoctoral Fellowship. L.T. was supported by a UTS Chancellor's Postdoctoral Fellowship.

REFERENCES

1. **Poole K.** 2011. *Pseudomonas aeruginosa*: resistance to the max. Front. Microbiol. **2:**65. http://dx.doi.org/10.3389/fmicb.2011.00065.
2. **Hamad B.** 2010. The antibiotics market. Nat. Rev. Drug Discov. **9:**675–676. http://dx.doi.org/10.1038/nrd3267.
3. **Kong KF, Schneper L, Mathee K.** 2009. Beta-lactam antibiotics: from antibiosis to resistance and bacteriology. APMIS **118:**1–36. http://dx.doi.org/10.1111/j.1600-0463.2009.02563.x.
4. **Bush K.** 2012. Antimicrobial agents targeting bacterial cell walls and cell membranes. Rev. Sci. Tech. **31:**43–56.
5. **Spratt BG, Cromie KD.** 1988. Penicillin-binding proteins of Gram-negative bacteria. Rev. Infect. Dis. **10:**699–711.
6. **Tomasz A.** 1986. Penicillin-binding proteins and the antibacterial effectiveness of beta-lactam antibiotics. Rev. Infect. Dis. **8**(Suppl 3)**:**S260–S278.
7. **Trautmann M, Heinemann M, Zick R, Moricke A, Seidelmann M, Berger D.** 1998. Antibacterial activity of meropenem against *Pseudomonas aeruginosa*, including antibiotic-induced morphological changes and endotoxin-liberating effects. Eur. J. Clin. Microbiol. Infect. Dis. **17:**754–760.
8. **Horii T, Kobayashi M, Sato K, Ichiyama S, Ohta M.** 1998. An in-vitro study of carbapenem-induced morphological changes and endotoxin release in clinical isolates of Gram-negative bacilli. J. Antimicrob. Chemother. **41:**435–442.
9. **Nishino T, Nakazawa S.** 1976. Bacteriological study on effects of beta-lactam group antibiotics in high concentrations. Antimicrob. Agents Chemother. **9:**1033–1042.
10. **Chadwick P.** 1969. Effect of carbenicillin on *Pseudomonas aeruginosa*. Can. Med. Assoc. J. **101:**74–80.
11. **Zar FA, Kany RJ, Jr.** 1985. In vitro studies of investigational beta-lactams as possible therapy for *Pseudomonas aeruginosa* endocarditis. Antimicrobial. Agents Chemother. **27:**1–3.
12. **Tam VH, Schilling AN, Melnick DA, Coyle EA.** 2005. Comparison of beta-lactams in counter-selecting resistance of *Pseudomonas aeruginosa*. Diagn. Microbiol. Infect. Dis. **52:**145–151. http://dx.doi.org/10.1016/j.diagmicrobio.2005.02.010.
13. **Burgess DS.** 2005. Use of pharmacokinetics and pharmacodynamics to optimize antimicrobial treatment of *Pseudomonas aeruginosa* infections. Clin. Infect. Dis. **40**(Suppl 2)**:**S99–S104. http://dx.doi.org/10.1086/426189.
14. **Tam VH, Schilling AN, Neshat S, Poole K, Melnick DA, Coyle EA.** 2005. Optimization of meropenem minimum concentration/MIC ratio to suppress in vitro resistance of *Pseudomonas aeruginosa*. Antimicrob. Agents Chemother. **49:**4920–4927. http://dx.doi.org/10.1128/AAC.49.12.4920-4927.2005.
15. **Palmer KL, Aye LM, Whiteley M.** 2007. Nutritional cues control *Pseudomonas aeruginosa* multicellular behavior in cystic fibrosis sputum. J. Bacteriol. **189:**8079–8087. http://dx.doi.org/10.1128/JB.01138-07.
16. **Clinical and Laboratory Standards Institute.** 2003. Methods for dilution antimicrobial susceptibility tests for bacteria that grow aerobically, 6th ed. Approved standard M7-A6. Clinical and Laboratory Standards Institute, Wayne, PA.
17. **Strauss MP, Liew AT, Turnbull L, Whitchurch CB, Monahan LG, Harry EJ.** 2012. 3D-SIM super resolution microscopy reveals a bead-like arrangement for FtsZ and the division machinery: implications for triggering cytokinesis. PLoS Biol. **10:**e1001389. http://dx.doi.org/10.1371/journal.pbio.1001389.
18. **Gustafsson MG, Shao L, Carlton PM, Wang CJ, Golubovskaya IN, Cande WZ, Agard DA, Sedat JW.** 2008. Three-dimensional resolution doubling in wide-field fluorescence microscopy by structured illumination. Biophys. J. **94:**4957–4970. http://dx.doi.org/10.1529/biophysj.107.120345.
19. **Watanakunakorn C, Hamburger M.** 1969. Induction of spheroplasts of *Pseudomonas aeruginosa* by carbenicillin. Appl. Microbiol. **17:**935–937.
20. **Justice SS, Hunstad DA, Cegelski L, Hultgren SJ.** 2008. Morphological plasticity as a bacterial survival strategy. Nat. Rev. Microbiol. **6:**162–168. http://dx.doi.org/10.1038/nrmicro1820.
21. **Fjell CD, Hiss JA, Hancock RE, Schneider G.** 2012. Designing antimicrobial peptides: form follows function. Nat. Rev. Drug Discov. **11:**37–51. http://dx.doi.org/10.1038/nrd359110.1038/nrd3591.
22. **Hancock REW, Nijnik A, Philpott DJ.** 2012. Modulating immunity as a therapy for bacterial infections. Nat. Rev. Microbiol. **10:**243–254. http://dx.doi.org/10.1038/nrmicro2745.
23. **Kapoor R, Wadman MW, Dohm MT, Czyzewski AM, Spormann AM, Barron AE.** 2011. Antimicrobial peptoids are effective against *Pseudomonas aeruginosa* biofilms. Antimicrob. Agents Chemother. **55:**3054–3057. http://dx.doi.org/10.1128/AAC.01516-10.
24. **Wright GD.** 2012. Antibiotics: a new hope. Chem. Biol. **19:**3–10. http://dx.doi.org/10.1016/j.chembiol.2011.10.019.
25. **Boucher HW, Talbot GH, Bradley JS, Edwards JE, Gilbert D, Rice LB, Scheld M, Spellberg B, Bartlett J.** 2009. Bad bugs, no drugs: no ESKAPE! An update from the Infectious Diseases Society of America. Clin. Infect. Dis. **48:**1–12. http://dx.doi.org/10.1086/595011.
26. **Piddock LJ.** 2012. The crisis of no new antibiotics—what is the way forward? Lancet Infect. Dis. **12:**249–253. http://dx.doi.org/10.1016/S1473-3099(11)70316-4.
27. **Ejim L, Farha MA, Falconer SB, Wildenhain J, Coombes BK, Tyers M, Brown ED, Wright GD.** 2011. Combinations of antibiotics and nonantibiotic drugs enhance antimicrobial efficacy. Nat. Chem. Biol. **7:**348–350. http://dx.doi.org/10.1038/nchembio.559.
28. **Lehar J, Zimmermann GR, Krueger AS, Molnar RA, Ledell JT, Heilbut AM, Short GF, 3rd, Giusti LC, Nolan GP, Magid OA, Lee MS, Borisy AA, Stockwell BR, Keith CT.** 2007. Chemical combination effects predict connectivity in biological systems. Mol. Syst. Biol. **3:**80. http://dx.doi.org/10.1038/msb4100116.
29. **Sharom JR, Bellows DS, Tyers M.** 2004. From large networks to small molecules. Curr. Opin. Chem. Biol. **8:**81–90. http://dx.doi.org/10.1016/j.cbpa.2003.12.007.
30. **Walsh C.** 2000. Molecular mechanisms that confer antibacterial drug resistance. Nature **406:**775–781. http://dx.doi.org/10.1038/35021219.
31. **Mesaros N, Nordmann P, Plesiat P, Roussel-Delvallez M, Van Eldere J, Glupczynski Y, Van Laethem Y, Jacobs F, Lebecque P, Malfroot A, Tulkens PM, Van Bambeke F.** 2007. *Pseudomonas aeruginosa*: resistance and therapeutic options at the turn of the new millennium. Clin. Microbiol. Infect. **13:**560–578. http://dx.doi.org/10.1111/j.1469-0691.2007.01681.x.
32. **Watanakunakorn C, Phair JP, Hamburger M.** 1970. Increased resistance of *Pseudomonas aeruginosa* to carbenicillin after reversion from spheroplast to rod form. Infect. Immun. **1:**427–430.
33. **Ryall B, Eydallin G, Ferenci T.** 2012. Culture history and population heterogeneity as determinants of bacterial adaptation: the adaptomics of a single environmental transition. Microbiol. Mol. Biol. Rev. **76:**597–625. http://dx.doi.org/10.1128/MMBR.05028-11.